Polymer 51 (2010) 92–99

Contents lists available at ScienceDirect

Polymer

journal homepage: www.elsevier.com/locate/polymer

Preparation and characterization of hyperbranched polymer grafted mesoporous silica nanoparticles via self-condensing atom transfer radical vinyl polymerization

Xin Li, Chun-Yan Hong*, Cai-Yuan Pan

CAS Key Laboratory of Soft Matter Chemistry, Department of Polymer Science and Engineering, University of Science and Technology of China, Hefei 230026, Anhui, PR China

ARTICLE INFO

Article history:
Received 24 July 2009
Received in revised form
18 October 2009
Accepted 2 November 2009
Available online 17 November 2009

Keywords:
Organic–inorganic hybrids
Hyperbranched polymer
SCATRVP

ABSTRACT

Hyperbranched poly(2-((bromobutyryl)oxy)ethyl acrylate) (HPBBEA) was grafted onto the exterior surface of mesoporous silica nanoparticles (MSNs) by surface-initiated self-condensing atom transfer radical vinyl polymerization (SCATRVP). The MSNs with ATRP initiator anchored on the exterior surface (MSN-Br) were prepared by the reaction of 5,6-dihydroxyhexyl-functionalized MSNs (MSN-OH) with α-bromoisobutyryl bromide. Afterwards, MSN-Br was utilized as initiator in the SCATRVP of inimer BBEA, resulting in core–shell nanoparticles with MSN core and HPBBEA shell (MSN-g-HPBBEA). The molecular weight of HPBBEA increased with the increasing ratio of BBEA to MSN-Br. In view of the high density of bromoester groups on the surface of HPBBEA shell, MSN-HPBBEA was used to initiate the successive polymerization of (2-dimethylamino-ethylmethacrylate) (DMAEMA), forming core–shell nanoparticles MSN-g-HPBBEA-g-PDMAEMA. The resultant products were characterized by FT-IR, NMR, HRTEM and thermogravimetric analysis (TGA), etc. The pH-responsive property of MSN-g-HPBBEA-g-PDMAEMA was characterized by measuring the hydrodynamics radius at different pH values, and this core–shell nanostructure may have potential applications in biomedicine and biotechnology.

1. Introduction

Mesoporous silica nanoparticles (MSNs) have attracted considerable interest in recent years due to their unique characters, such as stable mesoporous structure, high surface area, large pore volume, tunable pore size and non-toxicity; they are ideal materials for hosting molecules [1–7]. However, some major restrictions have not been resolved yet; MSNs have faint solubility in most organic and aqueous solvents, and their compatibility with chemical and biological systems need to be improved. Once these limitations can be solved, MSNs could be utilized in broad fields, such as synthetic scaffolds to mimic enzymes, molecular vessels and materials for controlled drug delivery [8].

In order to enhance the solubility and compatibility of MSNs, covalently attaching polymers onto the exterior surface of MSN has attracted considerable attention since this method could endow the surface of MSNs with novel properties. The procedure to anchor polymer chains to the surface was accomplished by either "grafting to" or "grafting from" techniques. The "grafting to" method means the coupling of preformed end-functionalized polymer chains the reactive surface groups on the MSNs [9], and the limitation is low grafting density of polymer chains. The "grafting from" method included attaching the initiating groups on the surface of MSNs and successively in situ surface-initiated polymerization. The advantage of this technique is easy preparation of MSNs with high density of polymer chains on their surface. By "grafting from" method, the polymers successfully grafted on the MSNs included poly(lactic acid) [10], polystyrene [11], poly(methyl methacrylate) [12] and smart polymers such as poly(acrylic acid) [13] and poly(*N*-isopropylacrylamide) (PNIPAAm) [14,15]. These polymers improved the solubility of MSNs and endued the surface of MSNs with some functionalities. The polymerization techniques reported included atom transfer radical polymerization (ATRP) [12,15], ring-opening polymerization (ROP) [10] and reversible addition-fragmentation chain transfer (RAFT) polymerization [11,13,14].

As mentioned above, the linear polymers have been used in the modification of MSNs, however, modification of MSNs with hyperbranched polymers was rarely reported. Compared to the linear polymers, hyperbranched polymers are special kinds of polymers with highly branched structure, they have good solubility, low melt viscosity, and extremely high density of functional groups, so they can be utilized advantageously as surface modifier and interfacial materials [16–19]. The hyperbranched polymers have similar properties to dendrimers while the synthesis is easier than that of dendrimers, so hyperbranched polymers played increasing important roles in industry and

* Corresponding author. Tel.: +86 551 3606081; fax: +86 551 3601592.
E-mail address: hongcy@ustc.edu.cn (C.-Y. Hong).

0032-3861/$ – see front matter © 2009 Elsevier Ltd. All rights reserved.
doi:10.1016/j.polymer.2009.11.020

laboratory [16]. Anchoring the hyperbranched polymers on the ZnO [20] and silica nanoparticles [21] has been studied for improving solubility of the inorganic materials, and the hybrid nanoparticles obtained exhibited some novel properties. In our previous report [22], the hyperbranched polymer was grafted onto carbon nanotubes for improving the solubility and processability of carbon nanotubes.

Although the grafting of hyperbranched polymer on silica nanoparticles have been studied [21], only few papers [23,24] investigated anchoring the hyperbranched polymers onto MSNs via ring-opening polymerization. Grafting hyperbranched polymers onto MSNs via surface ATRP has not been reported based on our knowledge. Special attention we must pay is grafting the hyperbranched polymers onto the exterior surface to ensure the pores not being filled with polymers. Herein, we report a convenient method to decorate the exterior surface of MSNs with hyperbranched polymers by surface-initiated SCATRVP of AB* inimer as shown in Scheme 1, where A and B* represent vinyl and initiating group, respectively. MSNs anchored with 2-bromoisobutyryl groups (MSN-Br) were utilized as polyfunctional initiator, and 2-((bromobutyryl)oxy) ethyl acrylate (BBEA) was used as inimer.

Moreover, Müller et al. reported that the multifunctionality of surface through SCATRVP could be achieved independent on the core shape of nanoparticles and the thickness of the polymer shell [21]. The hyperbranched polymers have high density of initiating groups that can initiate polymerization of different kinds of monomers [25], if the initiating sites initiate the polymerization of functional monomer, the functionalized MSNs might have some functionalities, such as environmentally sensitive property. Thus in the present paper, the MSN-g-HPBBEA was utilized as ATRP macroinitiator, to prepare the novel organic/inorganic hybrid material MSN-g-HPBBEA-g-PDMAEMA which has potential applications as stimuli responsive molecular vessels for hosting and controlled release of drugs, enzymes and DNAs.

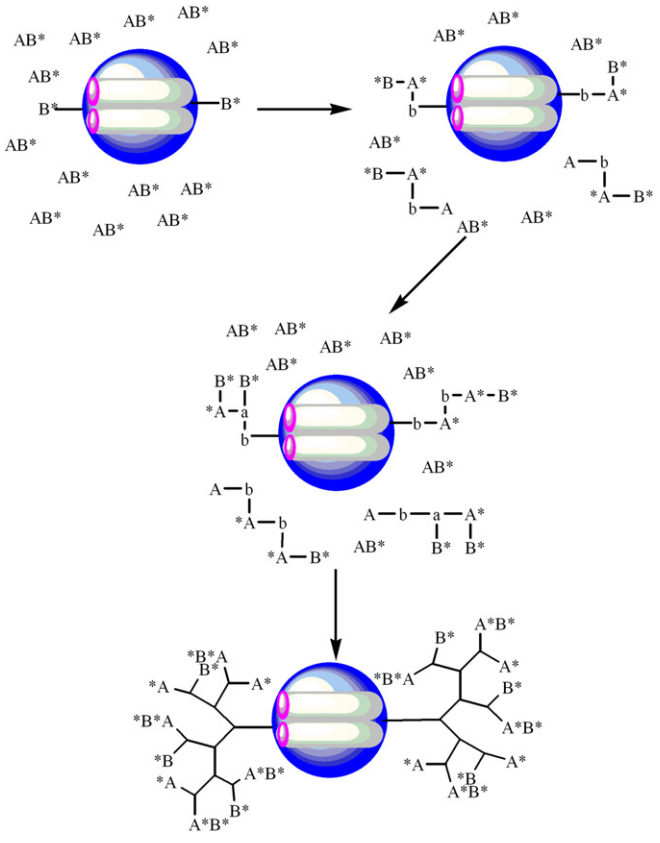

Scheme 1. Procedure of SCATRVP of inimer from MSN-Br.

2. Experimental section

2.1. Materials

Tetraethyl orthosilicate (TEOS, Aldrich, 98%), *n*-cetyltrimethylammonium bromide (CTAB, Aldrich, 98%), α-bromoisobutyryl bromide (BiBB, Aldrich), (2-dimethylamino) ethyl methacrylate (DMAEMA, Aldrich, 98%), 5,6-Epoxyhexyltriethoxysilane (EHTES, Gelest), 1,1,4,7,7-pentamethyldiethylenetriamine (PMDETA, Acros, 99%) were used as received. CuBr (Shanghai Chemical Reagent Co. analytical grade, 98%) was treated by glacial acetic acid, washed with methanol, and then dried in a vacuum oven. Toluene was refluxed with sodium under nitrogen and distilled. THF was distilled from a purple sodium ketyl solution. Triethyl amine (TEA) was dried by sodium hydroxide and distilled before use. 2-(((bromobutyryl)oxy) ethyl acrylate) (BBEA) was synthesized according to reference [22].

2.2. Characterization

^{1}H NMR spectra were recorded on a Bruker-300 MHz NMR instrument using $CDCl_3$ as solvent and tetramethylsilane as internal reference. Fourier transform infrared (FT-IR) spectra were recorded on a Bruker VECTOR-22 infrared spectrometer; the samples were mixed with KBr and then compressed into pellets. Thermogravimetric analysis (TGA) was carried out on a Perkin–Elmer TGA-7 instrument with a heating rate of 10°C/min under nitrogen. X-ray photoelectron spectroscopy (XPS) was carried out on ESCALAB MK II instrument. High resolution transmission electron microscope (HRTEM) images were recorded from JEOL JEM-2010 instrument. Molecular weights and molecular weight distributions were determined on a Waters 150C gel permeation chromatography (GPC) equipped with Ultrastyragel columns (10^3, 10^4 and 10^5 Å) and 410 refractive index detector at 30 °C, using monodispersed polystyrene as calibration standards. THF was used as eluent at a flow rate of 1.0 mL/min. Powder X-ray diffraction experiments were performed on a PHILIPS X'Pert PRO diffractometer using a CuK_α radiation source. Low angle diffraction with a 2θ range of 1–10° was used to investigate the long-range order of the materials. The surface area and median pore diameter were measured using N_2 adsorption/desorption measurements in a Micromeritics ASAP 2020 Accelerated Surface Area and Porosimetry. The data were evaluated using the BET and BJH methods to calculate the surface area and pore volume/pore size distributions, respectively. Elemental analysis was performed on Elementar Vario ELIII device. Hydrodynamics radius (R_h) of hybrid nanoparticles was characterized by Malvern Zetasizer Nano ZS90 with a He–Ne laser (633 nm) and 90° collecting optics.

2.3. Synthesis of mesoporous silica nanoparticles (MSNs)

The mesoporous silica nanoparticles (MSNs) were synthesized similar to the method reported by Lin et al. [10]. Aqueous solution of sodium hydroxide (2.0 M, 4 mL) was added dropwise to a solution of *N*-cetyltrimethylammonium bromide (CTAB) (1.0 g, 2.7×10^{-3} mol) in deionized water (500 mL), and into this solution at 80 °C, tetraethyl orthosilicate (TEOS, 5.00 mL, 2.5×10^{-2} mol) was then added dropwise. The mixture was stirred for 4 h. The white precipitates were obtained by filtration, washed with methanol, and dried in vacuum oven at 40 °C. The average diameter of MSNs is about 100 nm, and the average pore size is about 2 nm.

2.4. Preparation of 5,6-dihydroxyhexyl-coated MSN (MSN-OH)

MSNs (1.0 g), 5,6-epoxyhexyltriethoxysilane (EHTES, 1.0 g, 3.8×10^{-3} mol), toluene (100 mL) were added into a 250 mL round-bottom flask equipped with a magnetic bar. The reaction system was stirred under refluxing overnight under nitrogen. The resulting product was obtained after filtering and washing with methanol thoroughly, and then dried under vacuum for 8 h at room temperature. The CTAB was removed by refluxing 5,6-epoxyhexyl-coated MSNs in 150 mL methanol solution of hydrochloric acid (1.6 M) overnight; at the same time, the 5,6-epoxyhexyl groups on the surface of MSNs were transformed into 5,6-dihydroxyhexyl units. The resulting MSNs were washed thoroughly with methanol to remove the unreacted EHTES.

2.5. Anchoring ATRP functionalities onto the exterior surface of MSNs

MSN-OH (0.2 g) was first dispersed in 40 mL of dry THF by ultrasonic for 20 min. A solution of α-bromoisobutyryl bromide (4.6 g, 20 mmol) in 10 mL THF was added dropwise to the MSN-OH suspension in ice-water bath. The mixture was stirred at room temperature for 24 h under nitrogen. The ATRP initiator functionalized MSN (MSN-Br) was obtained by centrifuging, then it was washed successively with distilled water, methanol and diethyl ether, and dried under vacuum at 40 °C.

2.6. Surface-initiated SCATRVP of BBEA using MSN-Br as initiator

MSN-Br (30.0 mg), BBEA (3.75 g, 15.4 mmol), CuBr (5.0 mg, 0.036 mmol) and PMDETA (13.0 mg, 0.072 mmol) in 2 mL of toluene were added into a polymerization tube. After three freeze-evacuate-thaw cycles, the polymerization tube was sealed under vacuum, and then placed in an oil bath thermostated at 100 °C. The polymerization was stopped by cooling the tube to 25 °C, and the polymerization tube was opened to air. The mixture was diluted with 50 mL THF. After ultrasonicated for 30 min, and centrifugalized for 15 min, the crude product was obtained. The solid was washed with THF for four times and then methanol twice for removal of free polymer and a trace amount of copper salt. A white solid (54.0 mg) was obtained after dried under vacuum for 24 h.

2.7. ATRP of DMAEMA using HPBBEA-functionalized MSN as initiator

A representative example is as follows: MSN-g-HPBBEA (20.0 mg), CuBr(I) (6 mg, 0.042 mmol), PMDETA (15 mg, 0.084 mmol), DMAEMA (0.40 g, 1.27 mmol) and 2 mL THF were added into a polymerization tube. After three freeze-evacuate-thaw cycles, the polymerization tube was sealed under vacuum. The sealed tube was placed in oil bath thermostated at 60 °C for 8 h. The mixture was dissolved in 50 mL THF, and then centrifugalized for 15 min to obtain the crude product. After washing with THF-centrifugation for four times and washing with methanol-centrifugation two times, the PDMAEMA grafted MSN-g-HPBBEA (MSN-g-HPBBEA-g-PDMAEMA) was dried at 40 °C for 24 h under vacuum.

2.8. Cleaving grafted HPBBEA and HPBBEA-g-PDMAEMA from MSN

The cleaving experiment of MSN-g-HPBBEA was conducted according to the method reported by Li et al. [26] by utilizing HF to remove the MSN core. The method of cleaving HPBBEA-g-PDMAEMA from MSN is partly different from the method mentioned above, after treating with hydrofluoric acid, the mixture was neutralized by adding aqueous solution of sodium carbonate (1 mL, 5%) [27]. The solution was dialyzed with deionized water for 72 h while the water was replaced with fresh water every 6 h, and the copolymer was obtained by freeze-drying. The recovered HPBBEA and HPBBEA-g-PDMAEMA were then subjected to GPC and ^{1}H NMR analysis.

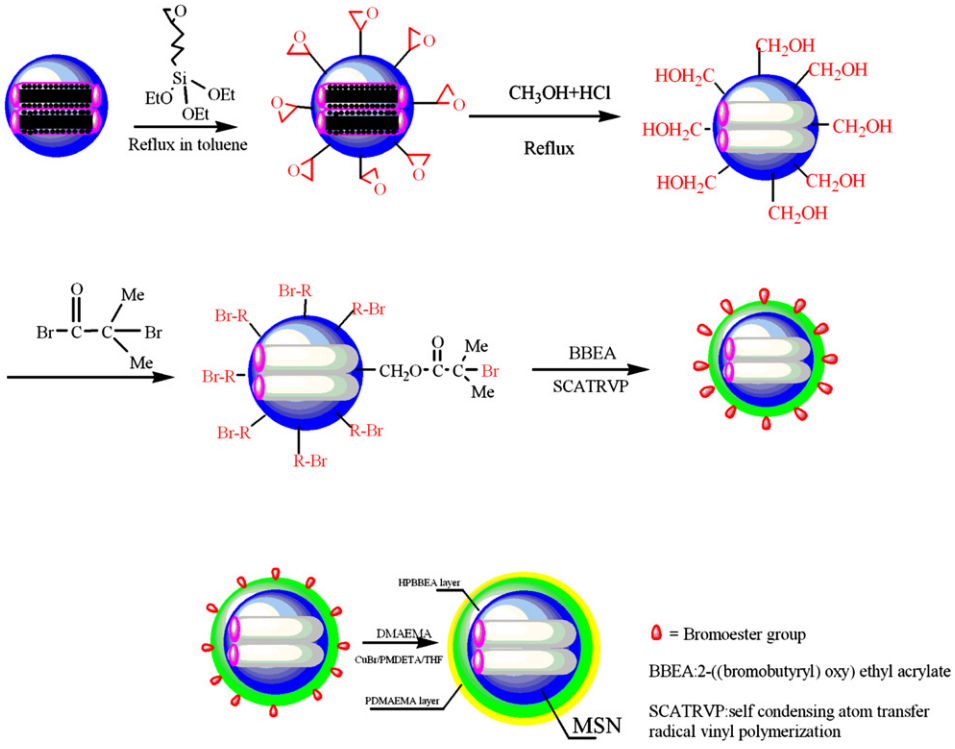

Scheme 2. The procedure for grafting hyperbranched polymer shell onto the exterior surface of MSN and ATRP of DMAEMA with MSN-g-HPBBEA as macroinitiator.

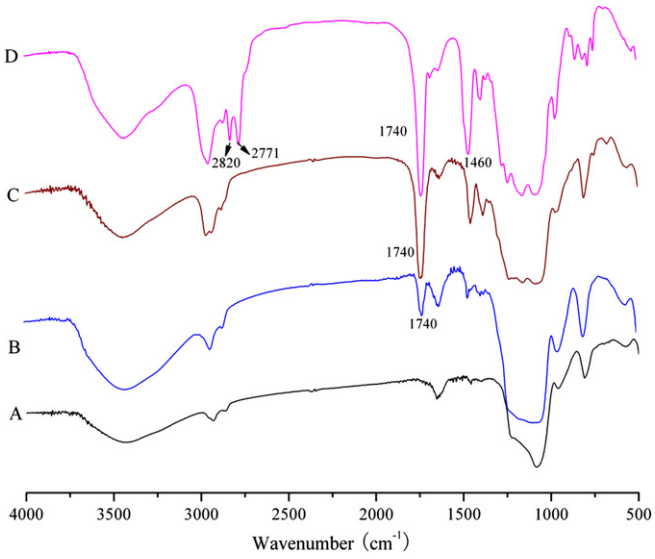

Fig. 1. FT-IR spectra of MSN-OH (A), MSN-Br (B) MSN-g-HPBBEA (C) and MSN-g-HPBBEA-g-PDMAEMA (D).

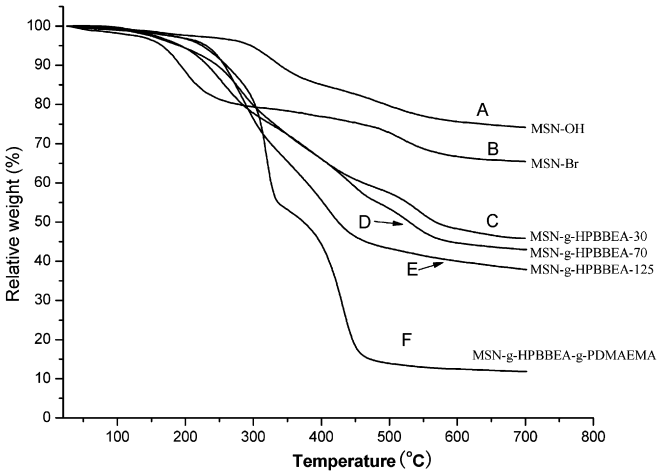

Fig. 3. TGA curves of MSN-OH (A), MSN-Br (B), and MSN-g-HPBBEA obtained from SCATRVP with different feed weight ratio of MSN-Br/BBEA, 1:30 (C); 1:70 (D); 1:125 (E) and MSN-g-HPBBEA-g-PDMAEMA (F).

3. Results and discussion

3.1. Immobilization of ATRP functionalities onto the exterior surface of MSNs

ATRP initiating groups were immobilized on mesoporous silica nanoparticles, as shown in Scheme 2. The significant issue in our experiment is to graft polymer chains onto the exterior surface of MSNs to ensure the pores not being filled with polymers. To achieve this, ATRP initiators must be anchored onto the exterior surface of MSNs. The MSNs with diameter of about 100 nm and average mesopore size of 2 nm were prepared by hydrolysis and polycondensation of TEOS in the presence of CTAB, and then MSNs with mesopores filled of CTAB reacted with EHTES under refluxing in toluene, forming EHTES-functionalized MSNs. Since the mesopores of MSNs were filled of CTAB, EHTES was grafted onto the exterior surface of MSNs, not interior surface of the mesopores. The resultant product was then refluxed in methanol solution of hydrochloric acid overnight to remove the CTAB template, and the epoxyhexyl groups were converted into 5,6-dihydroxyhexyl units [10]. ATRP initiators-functionalized MSNs (MSN-Br) were achieved by the reaction of 5,6-dihydroxyhexyl units with α-bromoisobutyryl bromide.

The ATRP initiator was immobilized on MSNs, which can be confirmed by FT-IR spectrum, as shown in Fig. 1B, besides the characteristic Si–O and C–H stretching vibrations at 1095 and 2933 cm^{-1}, a new absorbance band at 1740 cm^{-1} ascribed to C=O of bromoisobutyryl units has been observed.

X-ray photoelectron spectroscopy (XPS) analysis was utilized to characterize MSN-Br, and the result is shown in Fig. 2A. The major peak components at the binding energy (BE) of 533.10, 102.10 and 154.20 eV are assigned to O1s, Si2p and Si2s, respectively. The signals at 285.70 eV and 70.30 eV are attributable to C1s and Br3p of the bromoisobutyryl groups, respectively. The XPS results support the results of FT-IR, and the bromoisobutyryl groups were successfully anchored to the exterior surface of MSNs via the esterification of hydroxyl groups on MSNs with α-bromoisobutyryl bromide.

TGA curves of MSN-OH and MSN-Br in Fig. 3A and B show weight losses of 25% and 35%, respectively, which are ascribed to decomposition of organic groups and condensation of residual

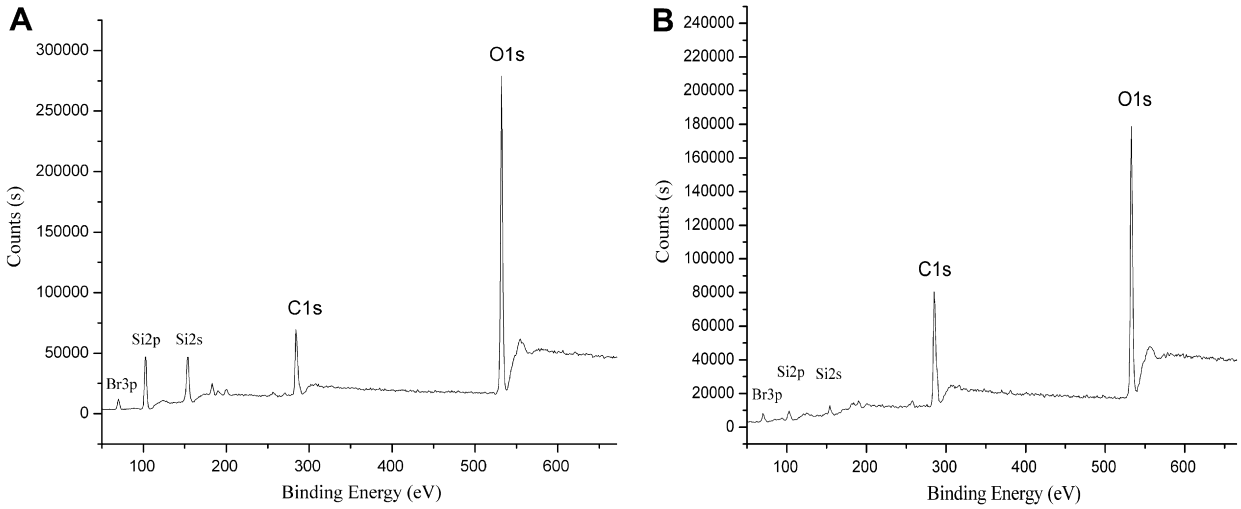

Fig. 2. The XPS spectra of MSN-Br (A) and MSN-g-HPBBEA (B).

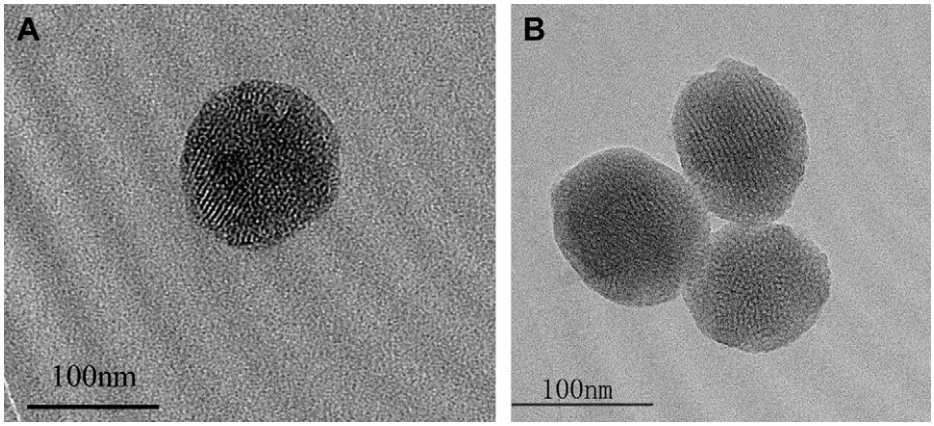

Fig. 4. HRTEM images of MSN-Br (A) and MSN-g-HPBBEA (B).

silanols [28]. Different from previous reports that the density of ATRP agents on the surface of silica nanoparticles can be calculated accurately [21], the density of ATRP initiating groups on the MSNs is not easy to be estimated due to many hatches of pores on the exterior surface of MSNs.

3.2. SCATRVP of BBEA using MSN-Br as initiator

SCATRVP of inimer BBEA was performed in the presence of MSN-Br at weight ratios of BBEA to MSN-Br being 30, 70 and 125, respectively. To achieve high conversions, the polymerizations lasted for 72 h at 100 °C.

In the polymerization system, both grafted and ungrafted polymers were produced because chain growth can be started not only from the B* groups immobilized on MSNs but also the B* groups in the inimers. The B* of MSN-Br is tertiary bromide group, its reactivity is higher than that of B* in the inimer BBEA, which is secondary bromide [21,29]. The concentration of inimer is much higher than that of MSN-Br, so formation of ungrafted polymer cannot be avoided. After the polymerization, the reaction mixture was diluted with THF and centrifugated, the product was washed with THF four times and methanol twice for removal of ungrafted HPBBEA and a trace amount of copper salt.

To confirm the grafting of HPBBEA onto MSNs, the sample was characterized by FT-IR. The result shown in Fig. 1C demonstrates that the characteristic C–H stretching vibrations between 2840 and 2970 cm^{-1} and carbonyl stretching band at 1740 cm^{-1} were strengthened, in comparison with the FT-IR spectrum of MSN-Br in Fig. 1B.

The XPS spectrum of MSN-g-HPBBEA is shown in Fig. 2B. Compare to the XPS spectrum of MSN-Br in Fig. 2A, the peak assigned to Si2p and Si2s became very weak, meanwhile, the peak of C1s became strong. The FT-IR and XPS results demonstrated that the HPBBEA was successfully grafted onto the surface of MSNs.

TGA was employed to estimate the weight loss of MSN-g-HPBBEA. As illustrated in Fig. 3, MSN-g-HPBBEA 30, MSN-g-HPBBEA 70 and MSN-g-HPBBEA 125, which were prepared from polymerization with feed weight ratios of BBEA to MSN-Br being 30, 70 and 125, lost their weights of 54%, 57% and 63%, respectively, which are much higher than that of MSN-Br (35%). Thus, the HPBBEA was successfully grafted onto MSN.

The HRTEM images of MSN-Br and MSN-g-HPBBEA 125 are shown in Fig. 4. In comparison with the HRTEM image of MSN-Br (Fig. 4A), MSN-g-HPBBEA nanoparticles (Fig. 4B) show polymer

Table 1
Nitrogen sorption isotherms of MSN-Br and MSN-g-HPBBEA.

Materials	BET surface areas (m^2/g)	BET pore volume (cm^3/g)	BJH average pore diameter (Å)
MSN-Br	770.31	0.83	22.9
MSN-g-HPBBEA	158.90	0.33	22.3

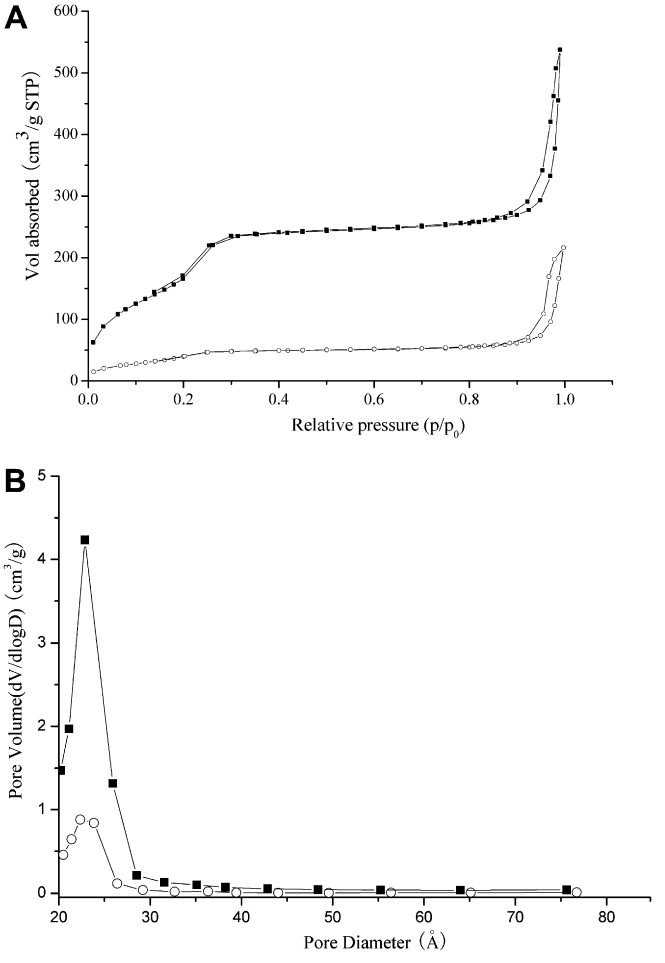

Fig. 5. BET nitrogen adsorption/desorption isotherms (A) and BJH pore size distributions (B) of MSN-Br and MSN-g-HPBBEA materials. (■: indicates MSN-Br, ○: indicates MSN-g-HPBBEA).

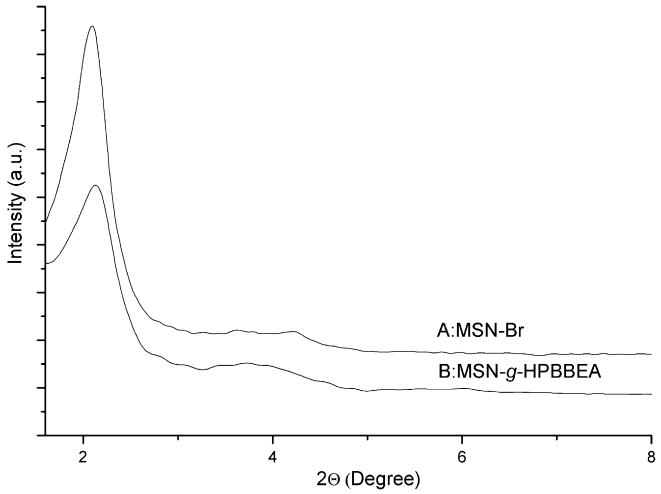

Fig. 6. Powder X-Ray diffraction patterns of MSN-Br (A) and MSN-g-HPBBEA (B).

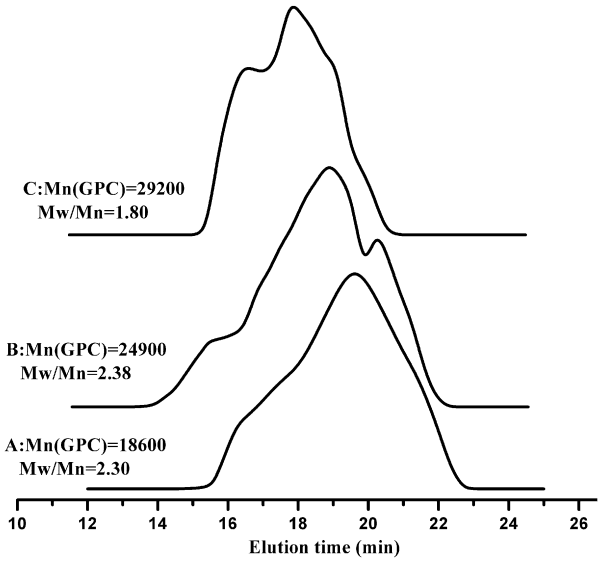

Fig. 8. GPC traces of HPBBEA cleaved from MSN-g-HPBBEA prepared from polymerization of BBEA at various feed weight ratios of BBEA to MSN-Br, A: 30, B: 70, C: 125.

shell; moreover, the honeycomb structure can be observed clearly in Fig. 4B, indicating the mesoporous structure of the core still remained after surface-initiated SCATRVP.

The N_2 sorption properties of MSN-Br and MSN-g-HPBBEA were measured. As listed in Table 1, the total surface areas and the average pore diameters of MSN-Br, MSN-g-HPBBEA were analyzed by the BET and BJH methods, respectively. The BET isotherms of these two materials exhibited the characteristic Type IV adsorption/desorption patterns, which indicated the presence of cylindrical channel-like porous structure (Fig. 5A). The decrease of surface areas is ascribed to the polymer grafting onto the outer surface of MSN [9]. The BJH analysis (Fig. 5B) of two materials exhibited narrow pore size distributions, which confirms that the mesopores remain accessible by nitrogen even after the polymerization [15].

The powder X-ray diffraction patterns of MSN-Br and MSN-g-HPBBEA were listed in Fig. 6, the intense (100) reflection peak corresponding to lattice spacing at $d = 4$ nm existed in MSN-Br and MSN-g-HPBBEA. The result demonstrates that the parallel cylindrical channel-like mesoporous structure of the MSN material was not demolished by the SCATRVP of BBEA [10,15].

The ^{1}H NMR spectrum of HPBBEA cleaved from the surface of MSNs is shown in Fig. 7. The signals at 4.1–4.5 ppm are ascribed to the ester ethylene of BBEA units and methine proton adjacent to bromide. The signals at 1.2–2.7 ppm correspond to the methylene and methine protons in the BBEA units in backbone of polymer, and methylene proton in butyrate groups. The signals in the region of 0.6–1.2 ppm could be attributed to methyl protons in butyrate groups [30].

GPC traces of hyperbranched polymer chains cleaved from MSN-g-HPBBEA are shown in Fig. 8. The M_ns of HPBBEA 30, HPBBEA 70 and HPBBEA 125 are 18 600, 24 900 and 29 200, respectively. It is understandable that the molecular weights of HPBBEA grafted on MSN increased with the increasing weight ratio of BBEA to MSN-Br from 30 to 125. GPC results in Fig. 8 show that all traces displayed multi-peak, and the molecular weight distributions (M_w/M_n) are broad, which are the universal phenomena for SCVP of inimers [21,30–33].

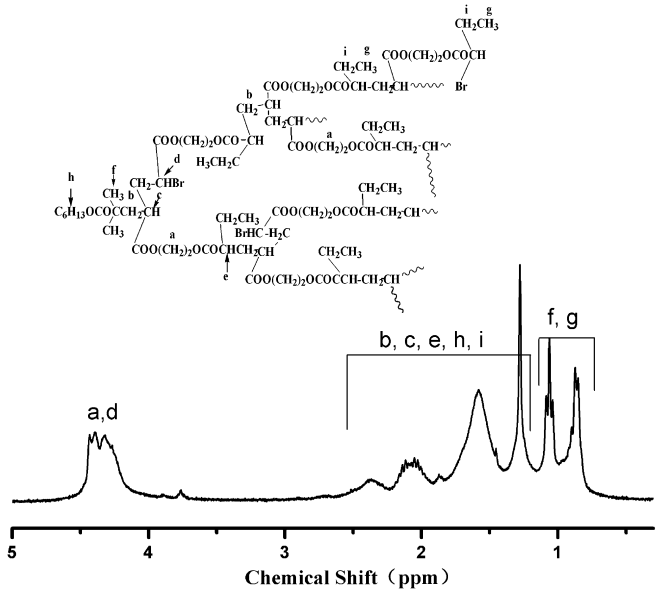

Fig. 7. ^{1}H NMR spectrum of HPBBEA cleaved from MSN-g-HPBBEA 125.

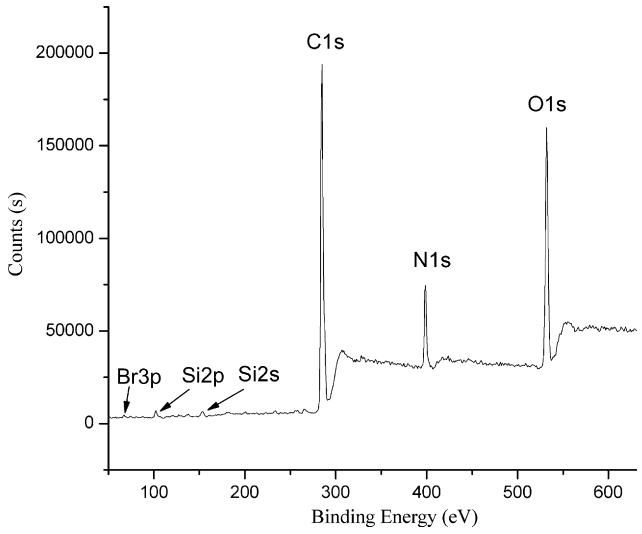

Fig. 9. The XPS spectrum of MSN-g-HPBBEA-g-PDMAEMA.

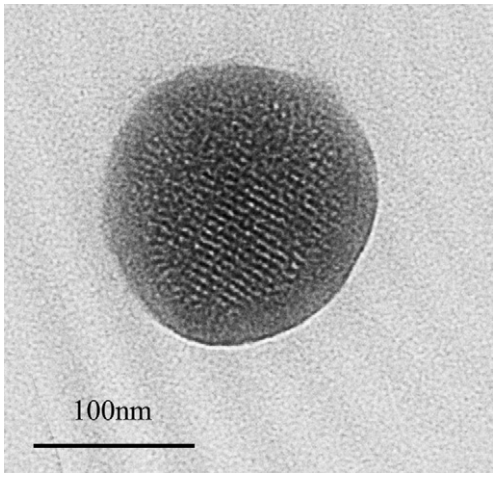

Fig. 10. HRTEM image of MSN-g-HPBBEA-g-PDMAEMA.

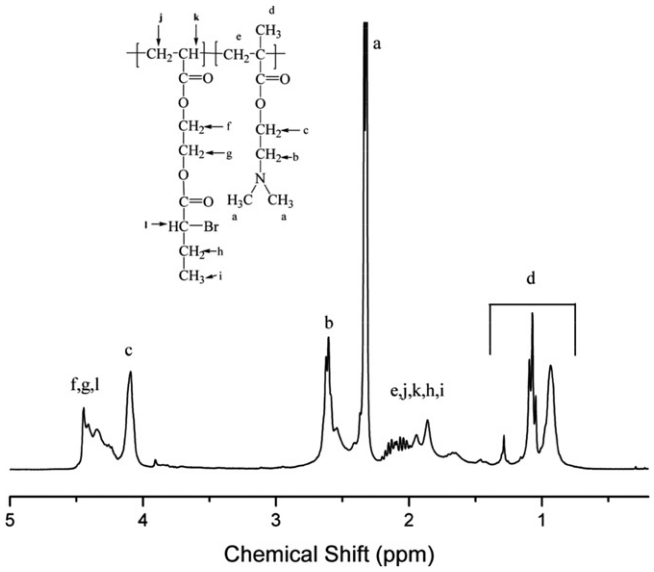

Fig. 11. ^{1}H NMR spectrum of HPBBEA-g-PDMAEMA cleaved from MSN-g-HPBBEA-g-PDMAEMA.

3.3. ATRP of DMAEMA with MSN-g-HPBBEA as macroinitiator

Since MSN-g-HPBBEA has high density of initiating groups on the surface, it can be used as macroinitiator for successive polymerization of various monomers. In this study, MSN-g-HPBBEA 125 was used as macroinitiator in the ATRP of DMAEMA; the polymerization was carried out at 60 °C for 8 h. The resultant MSN-g-HPBBEA-g-PDMAEMA was characterized by FT-IR. Compare to the FT-IR spectrum of MSN-g-HPBBEA in Fig. 1C, new bands of PDMAEMA appeared at 2820 cm^{-1} and 2771 cm^{-1} attributed to the C–H stretching of $-N(CH_3)_2$ [34] in Fig. 1D, ester carbonyl absorption band at 1740 cm^{-1} and C–H binding band at 1462 cm^{-1} are strengthened further. These results demonstrated that the PDMAEMA was grafted onto the surface of HPBBEA on the MSNs.

The XPS spectrum of MSN-g-HPBBEA-g-PDMAEMA is shown in Fig. 9. Compared with the XPS spectrum of MSN-g-HPBBEA (Fig. 2B), the peaks of Si2p, Si2s and Br3p became very weak, meanwhile, a new peak at 399.8 eV ascribed to N1s of PDMAEMA appeared, indicating that nanoparticles with the HPBBEA-g-PDMAEMA shell and MSN core were formed, and the polymer shell is so thick that the XPS technology cannot probe most Si element of the MSN core because probing depth of XPS is usually about 8–10 nm [35].

TGA was utilized to characterize the MSN-g-HPBBEA-g-PDMAEMA. The total weight loss was about 90%, which is much higher than that of MSN-g-HPBBEA 125, indicates that PDMAEMA was successfully grafted onto the HPBBEA hyperbranched polymer shell of composite nanoparticles.

The HRTEM image of MSN-g-HPBBEA-g-PDMAEMA is shown in Fig. 10. The core–shell structure can be clearly observed, and the thickness of the shell is about 20 nm in average, which is higher than that of MSN-g-HPBBEA (Fig. 4B). Meanwhile the honeycomb structure of MSN is obvious in Fig. 10, which illustrates that the mesoporous structure remained after the polymerizations.

The HPBBEA-g-PDMAEMA was cleaved from the hybrid mesoporous silica particles using the method mentioned above [27]. ^{1}H NMR was employed to characterize the structure of the HPBBEA-g-PDMAEMA. As shown in Fig. 11, besides the signals of HPBBEA, the new signals at 2.3 and 2.6 ppm are ascribed to the methyl and methylene groups next to nitrogen atom in PDMAEMA, respectively. The signal at 4.1 ppm is ascribed to the ester methylene group of PDMAEMA [36]. ^{1}H NMR result illustrated the successfully grafting of PDMAEMA on the surface of hyperbranched polymer.

The molar ratio of HPBBEA and PDMAEMA in the copolymer can be calculated based on the ^{1}H NMR data of HPBBEA-g-PDMAEMA according to Eq. (1).

$$N_{\mathrm{HPBBEA}} : N_{\mathrm{PDMAEMA}} = \frac{2I_{4.2-4.5}}{5I_{4.1}} \quad (1)$$

$I_{4.1}$ is the integration of the signal at $\delta = 4.1$ ppm; $I_{4.2-4.5}$ is the integration of signals at $\delta = 4.2$–4.5 ppm. The molar ratio of HPBBEA and PDMAEMA is about 1:2.73. To further validate the ratio of HPBBEA to PDMAEMA, the elemental analysis was utilized to give the weight ratio of C:H:N in the copolymer, the molar ratio of HPBBEA and PDMAEMA calculated from elemental analysis is 1:2.96, which is similar to the value calculated from ^{1}H NMR.

The GPC trace of HPBBEA-g-PDMAEMA is shown in Fig. 12. The M_n of HPBBEA-g-PDMAEMA is 39 200 and the polydispersity index (PDI) is 1.14. The M_n of HPBBEA-g-PDMAEMA was higher than that of HPBBEA cleaved from MSN-g-HPBBEA.

The hydrodynamic radius (R_h) of the hybrid nanoparticles MSN-g-HPBBEA-g-PDMAEMA is plotted against pH values of aqueous solution (Fig. 13). The radius decreased with increase of pH values, and the sharp decrease of R_h was observed when pH values increased from 1 to 5.2, which illustrated the MSN-g-HPBBEA-g-

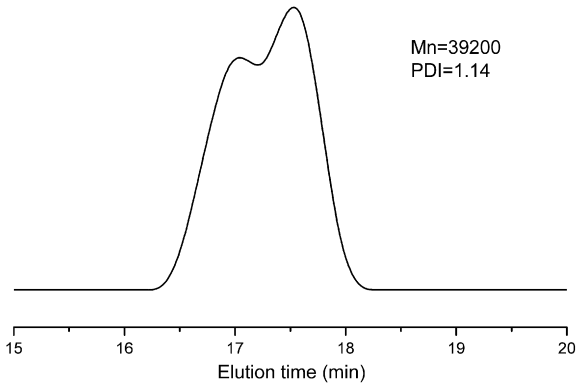

Fig. 12. GPC trace of HPBBEA-g-PDMAEMA cleaved from MSN-g-HPBBEA-g-PDMAEMA.

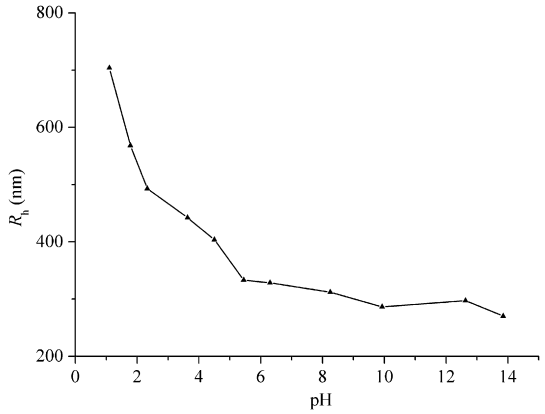

Fig. 13. R_h of MSN-g-HPBBEA-g-PDMAEMA in different pH.

PDMAEMA is sensitive to pH of solution. PDMAEMA is a weak electrolyte (pKa ≈ 7.3) [37], at low pH, such as pH = 1, PDMAEMA is entirely protonated to form polyelectrolyte with positive charge, and the polymer chains are extending fully due to the electrostatic repulsions between PDMAEMA chains. As a result, large R_h of the hybrid nanoparticles was obtained. Nevertheless, PDMAEMA chains were deprotonated and then became hydrophobic at high pH, so the polymer chains were collapsed and the R_h of the nanoparticles decreased.

Dispersion of MSN-Br into organic solvents and aqueous solution was very difficult, and sedimentation of MSN-Br from THF appeared in a few minutes after sonication. However, the MSN-g-HPBBEA was well dispersed in THF, chloroform and toluene. After the grafting of PDMAEMA on MSN-g-HPBBEA, the MSN-g-HPBBEA-g-PDMAEMA dispersed well in water, THF and chloroform. The good dispersibility of MSN-g-HPBBEA and MSN-g-HPBBEA-g-PDMAEMA make them attractive for further applications.

4. Conclusion

Core–shell nanostructure with a mesoporous silica nanoparticle core and a hyperbranched polymer shell has been prepared by the surface-initiated SCATRVP of BBEA using MSN with bromoisobutyryl groups as initiator. The molecular weight of HPBBEA grafted increased with the increasing ratio of inimer BBEA to MSN-Br. Hybrid nanoparticles showed better dispersibility in organic solvents than the precursor MSNs.

Utilizing MSN-g-HPBBEA as macroinitiator, PDMAEMA was successfully grafted onto the hyperbranched polymer shell of MSN-g-HPBBEA. The resultant nanoparticles, MSN-g-HPBBEA-g-PDMAEMA showed pH-responsive property, which will have potential applications in biomedicine and biotechnology.

Acknowledgement

This research was supported by National Natural Science Foundation of China (No. 20674077) and Program for New Century Excellent Talents in University (NCET-08-0520).

References

[1] Vallet RM, Ramila A, del Real RP, Perez PJ. Chem Mater 2001;13:308.
[2] Xue JM, Shi M. J Control Release 2004;98:209.
[3] Lai CY, Trewyn BG, Jeftinija DM, Jeftinija K, Xu S, Lin VSY, et al. J Am Chem Soc 2003;125:4451.
[4] Radu DR, Lai CY, Jeftinija K, Rowe EW, Jeftinija S, Lin VSY. J Am Chem Soc 2004;126:13216.
[5] Song SW, Hidajat K, Kawi S. Langmuir 2005;21:9568.
[6] Czaun M, Rahman MM, Takafuji M, Ihara H. Polymer 2008;49:5410.
[7] Chen ST, Guo CY, Liu L, Xu H, Dong JX, Hu YL. Polymer 2005;46:11093.
[8] De M, Ghosh PS, Rotello VM. Adv Mater 2008;20:4225.
[9] You YZ, Kalebaila KK, Brock SL, Oupicky D. Chem Mater 2008;20:3354.
[10] Radu DR, Lai CY, Wiench JW, Pruski M, Lin VSY. J Am Chem Soc 2004;126:1640.
[11] Hong CY, Li X, Pan CY. Eur Polym J 2007;43:4114.
[12] Audouin F, Blas H, Pasetto P, Beaunier P, Save M, Charleux B, et al. Macromol Rapid Commun 2008;29:914.
[13] Hong CY, Li X, Pan CY. J Mater Chem 2009;19:5155.
[14] Hong CY, Li X, Pan CY. J Phys Chem C 2008;112:15320.
[15] Chung PW, Kumar R, Pruski M, Lin VSY. Adv Funct Mater 2008;18:1390.
[16] Gao C, Yan D. Prog Polym Sci 2004;29:183.
[17] Matyjaszewski K, Pyun J, Gaynor SG. Macromol Rapid Commun 1998;19:665.
[18] Ambade AV, Kumar A. Prog Polym Sci 2000;25:1141.
[19] Cheng GL, Simon PFW, Hartenstein M, Muller AHE. Macromol Rapid Commun 2000;21:846.
[20] Liu P, Wang TM. Polym Eng Sci 2007;47:296.
[21] Mori H, Seng DC, Zhang MF, Muller AHE. Langmuir 2002;18:3682.
[22] Hong CY, You YZ, Wu DC, Liu Y, Pan CY. Macromolecules 2005;38:2606.
[23] Rosenholm JM, Duchanoy A, Linden M. Chem Mater 2008;20:1126.
[24] Rosenholm JM, Penninkangas A, Linden M. Chem Commun 2006;37:3909.
[25] Mu B, Wang TM, Liu P. Ind Eng Chem Res 2007;46:3069.
[26] Li C, Benicewicz BC. Macromolecules 2005;38:5929.
[27] Nagase K, Kobayashi J, Kikuch A, Akiyama Y, Kanazawa H, Okano T. Biomacromolecules 2008;9:1340.
[28] Casasus R, Marcos MD, Martinez MR, Ros-Lis JV, Soto J, Villaescusa LA, et al. J Am Chem Soc 2004;126:8612.
[29] Wang JS, Matyjaszewski K. Macromolecules 1995;28:7901.
[30] Hong CY, Pan CY. Polymer 2001;42:9385.
[31] Yan D, Muller AH, Matyjaszewski K. Macromolecules 1997;30:7015.
[32] Hong CY, Pan CY, Huang Y, Xu ZD. Polymer 2001;42:6733.
[33] Hong CY, Zou YF, Pan CY. Polym Int 2003;52:257.
[34] Roy D, Knapp JS, Guthrie JT, Perrier S. Biomacromolecules 2008;9:91.
[35] Tan KL, Woon LL, Wong HK, Kang ET, Neoh KG. Macromolecules 1993;26:2832.
[36] Liu T, Jia S, Kowalewski T, Matyjaszewski K, Casado PR, Belmont J. Macromolecules 2005;39:548.
[37] An SW, Thirtle PN, Thomas RK, Baines FL, Billingham NC, Armes SP, et al. Macromolecules 1999;32:2731.